



An Ensemble-Based Coastal Flooding Index For Early Warning Applications

Chiara Favaretto^{1,*}, Francesco Barbariol^{2,*}, Alvise Benetazzo², Luigi Cavaleri², Francesco Marcello Falcieri², Christian Ferrarin², Rossella Ferretti^{3,4}, Stefano Menegon², Matteo Nastasi^{3,4}, Gianluca Redaelli^{3,4}, Antonio Ricchi^{3,4}, Piero Ruol¹

¹ Department of Civil, Environmental and Architectural Engineering (DICEA), University of Padua, Padua, Italy

² Institute of Marine Sciences (ISMAR), Italian National Research Council (CNR), Venice, Italy

³ Center of Excellence Telesensing of Environment and Model Prediction of Severe events, University of L'Aquila, L'Aquila, Italy

⁴ Department of Physical and Chemical Sciences (DSFC), University of L'Aquila, L'Aquila, Italy

* These authors contributed equally to this work

Correspondence to: Francesco Barbariol (francesco.barbariol@cnr.it)

Abstract. Coastal flooding poses a major threat to low-lying coastal areas, particularly under increasing storm intensity and sea-level rise. Early warning systems traditionally rely on deterministic forecasts, which provide a single possible scenario and fail to represent forecast uncertainty. In this study, we evaluate a probabilistic early warning framework for coastal flooding based on short-range ensemble forecasts and assess the feasibility of ensemble reduction to support operational applications. A *Coastal Flooding Index (CFI)* is introduced, linking the total sea levels at the beach, computed by an atmosphere-ocean-wave modelling chain including nearshore wave processes, to the geometry of local coastal defences. The framework is applied as a pilot case to a low-lying, urbanized coastal stretch in the northern Adriatic Sea (Italy) and tested during two severe storm events (*Vaia*, 2018, and *Detlef*, 2019). Ensemble forecasts derived from a full atmospheric ensemble (50 members) are compared with a reduced ensemble (15 members) obtained through a clustering-based selection of representative members. Results show that the reduced ensemble consistently preserves the key probabilistic properties of the full ensemble, including the spatial patterns, timing, and magnitude of ensemble mean and spread of wind speed, significant wave height, nearshore sea level, and derived flooding indicators, while considerably reducing the computational cost (30% of numerical simulations required). Although limited to two events and a single site, this study demonstrates the potential of combining *CFI* with ensemble reduction to retain the benefits of probabilistic forecasting for coastal flooding early warning within operational constraints.

1 Introduction

Coastal hazards have the potential to cause significant damage to coastal communities, particularly in low-lying areas characterized by high population density and substantial environmental or economic value. In view of the impacts of climate change, particularly sea-level rise, the frequency of extreme marine events is expected to increase, leading to a higher likelihood of hazardous phenomena, such as coastal flooding (IPCC, 2023). In this context, effective adaptation strategies must include both long-term territorial planning, such as the design and implementation of coastal defence measures, and short-term



risk mitigation tools, among which Early Warning Systems (EWS) are crucial to accurately forecast and effectively communicate hazardous events in order to prevent people and assets from being unprepared (Chondros et al., 2021). In fact, EWS are fundamental to support civil protection activities prior to the occurrence of extreme marine events (Turner et al., 2024). In their comprehensive study, Chatzistratis et al. (2025) presented an inventory of the existing European EWS for coastal floods and their operational/technical specifications. Their analysis revealed a fragmented/inconsistent landscape, despite the clear requirement by end users for high-resolution and impact-based products. To be effective, such systems must be tailored to specific coastal hazards, such as flooding or erosion, by means of Early Warning Indices (EWI) that integrate meteo-marine variables (e.g., waves and sea levels) with site-specific coastal features (e.g., morphology, protection systems, and land use type), improving the reliability of impact forecasts. Harley et al. (2016) proposed two storm impact indicators, one applicable to stretches of coastline with natural dunes and one to locations with beachfront infrastructure. Both indicators are a measure of the amount of dry beach available between the model-derived waterline and the seaward edge of dunes or buildings. The USGS Total Water Level and Coastal Change Forecast Viewer is currently implementing an index that compares the total water level to the local dune features to determine the occurrence of dune erosion, overwash, and inundation/flooding (<https://coastal.er.usgs.gov/hurricanes/research/twlviewer/>). However, accurately predicting coastal hazards often requires more than a single deterministic forecast, which represents only one possible evolution of the meteorological and marine conditions and may therefore fail to capture the full range of plausible scenarios associated with highly variable storm events. For early warning applications, this limitation can reduce the reliability of impact assessments and the effectiveness of protective measures. The uncertainty in the simulation of sea storms, mostly associated to the atmospheric forcing and particularly to wind, can instead be addressed using ensemble modelling, which allows for the forecasting of both the expected coastal sea levels and the probability of critical alerting levels. Biolchi et al. (2022) proposed a semi-probabilistic coastal EWS relying on a multi-model ensemble, where the uncertainty is managed with a pool of different models rather than within a set of plausible scenarios produced by the same model. Such probabilistic information is crucial for enhancing preparedness, supporting emergency actions, and improving coastal management strategies (World Meteorological Organization, 2015; United Nations, 2022; Favaretto et al., 2024).

In the present study, an EWI specifically designed for coastal flooding alerts is evaluated: the *Coastal Flooding Index (CFI)*. *CFI* compares the total water level (TWL) with the berm and crest elevations of local coastal defences (e.g., dunes, seawalls, and promenades). The proposed index is tested in a pilot site located along the Northern Adriatic coast of Italy, Jesolo. The novelty of the proposed EWI lies in its use of short-range (48 hours) ensemble numerical forecasts derived from a coupled atmospheric–marine modelling chain, including the WRF atmospheric model, the SHYFEM hydrodynamic model, the WAVEWATCHIII (WW3) spectral wave model, and the XBeach hydro-morphodynamic model. While SHYFEM and WW3 provide sea-level and wave conditions nearshore, XBeach explicitly quantifies the wave contribution (wave set-up and run-up/run-down) to the total sea level at the beach, providing a more comprehensive assessment of coastal flooding potential with respect to using bulk estimation formulas (e.g., Stockdon et al, 2006).



In the context of operational early-warning applications, it is crucial that the ensemble modelling chain can be executed reliably within the time constraints required for real-time forecasting. Ensuring operational feasibility is of paramount importance, and an ensemble reduction is herein adopted, verifying if the accuracy in reproducing forecast intensity and probability is maintained also with respect to the EWI. The scope of ensemble reduction is to work with a smaller number of members with respect to a full atmospheric ensemble, still preserving the probabilistic information brought by the ensemble at a sufficient level, that is, keeping the probability distribution of the reduced ensemble (herein called RENS) as close as possible to that of the full ensemble (herein called ENS). Molteni et al (2001) have called this feature, the relevance of a RENS. A relevant RENS allows to reduce the computational effort needed to run operational probabilistic forecasting, leaving the opportunity to add model complexity (e.g., coupling Earth System Model components, using more sophisticated parameterisations) or to increase the grid resolution in local target areas. Thus, we intercompare the forecasts and the warnings obtained following the ensemble, reduced ensemble and deterministic approaches to highlight the benefits of the first two with respect to the third and to assess the effect of ensemble reduction on the modelling chain results and on the *CFI*.

The following sections set the stage describing the study area and the storm events considered (Section 2), the proposed EWI, the modelling framework and the ensemble reduction (Section 3). Afterwards, the results for the Jesolo pilot case are presented (Section 4) and discussed (Section 5), before concluding with some remarks in the perspective of an implementation of the proposed index in an operational pipeline (Section 6).

2 Pilot Case

The pilot case study focuses on the sandy coastal stretch between the mouths of the Piave and Sile rivers, located entirely within the municipality of *Jesolo* (Veneto Region, Italy; Figure 1). This area is characterized by intense tourism, attracting an average of five million visitors during the summer season (Maragno et al., 2023). The littoral faces the Northern Adriatic Sea, where two main wind regimes dominate: the south-easterly, warm and moist Sirocco, and the north-easterly, cold Bora winds, blowing along the major and minor axes of the basin, respectively. The Northern Adriatic Sea is frequently affected by storm surge events, mainly driven by strong Sirocco winds (Umgiesser et al., 2022).

The Jesolo coastal stretch is highly vulnerable to erosion, particularly in its north-eastern sector, and to coastal flooding. Since the 1950s, rapid urban expansion has occurred near the shoreline, resulting in the loss of the pre-existing dune system. The shoreline is currently stabilized by a series of permeable groins that partially intercept the intense longshore sediment transport directed from northeast to southwest. Coastal flood protection is ensured by a fragmented system comprising small seawalls, promenades, stepped revetments, and limited sections of dunes and levees. Several topographic and bathymetric datasets are available for the area, including a high-resolution Digital Terrain Model (DTM) and bathymetric surveys acquired in 2022 (Regione del Veneto, 2023). These data allow for a detailed characterization of both the nearshore zone and the elevation and geometry of the existing coastal defence structures. Figure 1 shows the study area and the existing types of coastal flood defences (i.e., the 7 structures listed in Figure 1 caption).

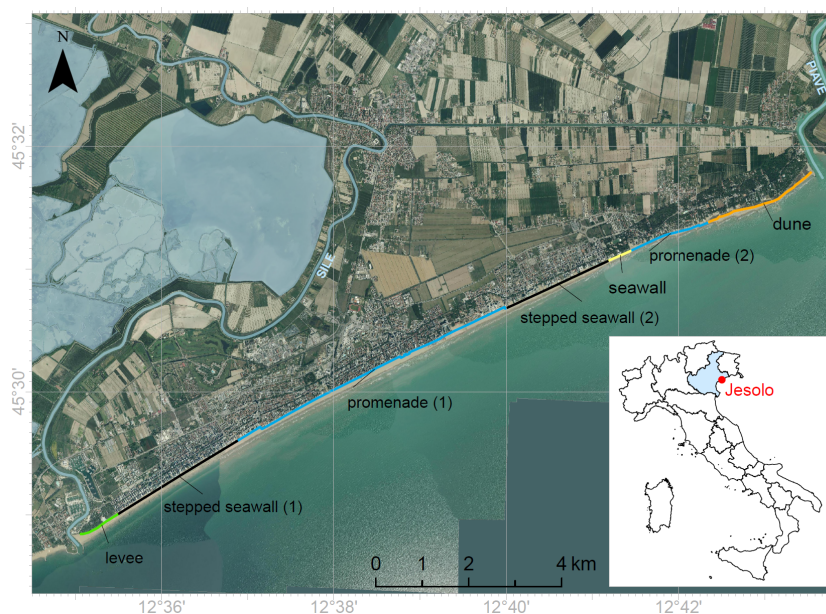


Figure 1: Pilot case study area of Jesolo (Italy): a low-lying sandy beach and urbanized territory facing the Northern Adriatic Sea. The different coastal defence structures protecting the shoreline between the Sile (left) and Piave (right) river mouths are highlighted in different colours (levee: green; stepped seawall: black; promenade: cyan; sea wall: yellow; dune: orange). Base map derived from the 2021 orthophoto provided by the Veneto Region (Italy)

The pilot case focuses on evaluating the EWI under two extreme storm events, *Vaia* (2018) and *Detlef* (2019), that seriously affected the study area. On October 29, 2018, a severe storm developed as a consequence of explosive cyclogenesis in the western Mediterranean Sea (Cavaleri et al., 2019). A strong south-easterly Sirocco wind persisted for several hours along the Adriatic Sea, generating extreme wave conditions (significant wave height H_s up to almost 6 m at the Acqua Alta Oceanographic Tower (AAOT), 8NM offshore the Jesolo shore) and elevated sea levels (1.21 m above msl at AAOT during the storm peak). This marine storm caused extensive damage along the Veneto coastline. In particular, the north-eastern sector of the Jesolo shoreline experienced dune erosion and complete inundation of the emerged beach (Figure 2a). On November 12, 2019, another severe storm event impacted the Venetian littoral, characterized by high waves and exceptional sea levels (Cavaleri et al., 2020). The water level reached 1.52 m above msl (measured at AAOT), resulting from the coincidence of an astronomical tidal peak with a severe storm surge generated by strong winds (up to 30 m/s) and a sudden pressure drop to 987 hPa. Along the Venetian coast, widespread flooding and structural damage were reported. In Jesolo, localized shoreline erosion and coastal flooding occurred, inundating the city center and several accommodation facilities (Figure 2b and c).



Figure 2: Impact of the extreme marine storms *Vaia* and *Detlef* on the pilot site: a) Emerged beach in the north-eastern part of the Jesolo coastline during the October 29, 2018 event; b) Flooding of Piazza Mazzini, Jesolo during the November 12, 2019 event; c) Flooding of the emerged beach along the Jesolo coastline (Consorzio Manzoni area) during the November 12, 2019 event.

3 Methodology

3.1 Coastal Flooding Index (CFI)

A relevant variable in coastal areas is the total sea level at the beach (Leijala et al., 2018), since it can be directly compared with the height of local coastal defences. The total sea level at the beach, $h_{TOT}(t)$, depends on both the sea level $h(t)$ and the wave-related contribution $h_w(t)$. The sea level $h(t)$ is the sum of the astronomical tide (z_A), the meteorological contribution (z_M), and the mean sea level (msl), which, as highlighted by Caruso & Marani (2022), accounts for long-term variations in water levels due to climate change and subsidence. The wave contribution $h_w(t)$ is given by the sum of the wave set-up $s(t)$ and the wave run-up/run-down $R(t)$, both of which depend on nearshore wave parameters and beach slope.

For the present study, two total sea level values, h_1 and h_2 (Figure 3), were defined and evaluated on an hourly basis:

- h_1 , the *total sea level for overtopping*, is defined as the sum of the hourly sea level h and the wave run-up $R_{up,2\%}$, i.e., the maximum onshore elevation reached by waves relative to the still-water shoreline position in the absence of waves (the 2% exceedance level). This value includes both wave set-up and swash uprush components:

$$h_1 = h + R_{up,2\%} \quad (1)$$

- h_2 , the *total sea level for overflow*, is defined as the sum of the hourly sea level h and the hourly average of set-up, run-up, and run-down contributions, i.e., $\langle h_w \rangle$, thus neglecting the swash component.

$$h_2 = h + \langle h_w \rangle \quad (2)$$



The two values were introduced to distinguish between different flooding mechanisms. Specifically, h_1 represents *wave*
 140 *overtopping* conditions, occurring when only the highest wave run-ups (swash) overcome the coastal defences. In contrast, h_2
 represents *overflow* conditions, associated with combined sustained high water levels and wave set-up, which increase the
 mean sea level near the coast and flood the protected areas behind the coastal defences. Cabrita et al. (2024) have stressed the
 difference in temporal characteristics of these variables naming them total water level (TWL) dynamic (h_1 , because of the
 episodic overtopping caused by the extreme run-up) and TWL static (h_2 , because the overflow is associated to the persistence
 145 of the mean water level above the structure crest height).

To define the *CFI*, these variables are compared to the characteristic of the local defence: h_c is the coastal defence
 crest height, h_B is the coastal defence berm height evaluated at the toe of the dune or of the local defence (Figure 3). Defining
 $\beta = h_1 - h_B$ as the *flooding parameter* (i.e., $\beta \geq 0$ indicated flooding), $\tau = h_c - h_B$ as the *relative coastal defence height*
 and $\alpha = h_1 - h_2$ as the contribution due to *swash uprush*, the *CFI* is expressed as:

150

$$\begin{cases} CFI = 0, & \text{if } \beta < 0 & \text{no flooding} \\ CFI = 1, & \text{if } 0 \leq \beta < \tau & \text{flooding of the emerged beach} \\ CFI = 2, & \text{if } \beta \geq \tau \text{ and } \beta - \alpha < \tau & \text{limited inland flooding due to wave overtopping} \\ CFI = 3, & \text{if } \beta \geq \tau \text{ and } \beta - \alpha \geq \tau & \text{inland flooding due to overflow} \end{cases} \quad (3)$$

taking integer values between 0 and 3 that can be associated to different levels of alert (0: no flooding, with $\beta < 0$; from 1 to
 3: different kind of flooding). The subdivision of the class with $\beta \geq \tau$ is intended to highlight whether the occurrence of inland
 flooding is primarily due to the presence of high waves that occasionally overtop the local defence ($\beta - \alpha < \tau$), or whether the
 155 local defence is overflowed due to solely high sea levels and wave set-up causing extensive flooding ($\beta - \alpha \geq \tau$).

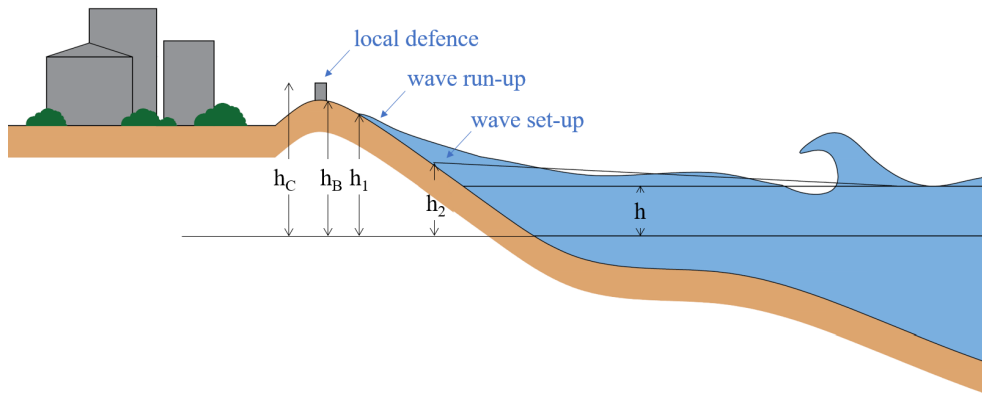


Figure 3: Scheme of the water levels h and coastal defence heights used for the *CFI* definition. h_c is the coastal defence crest height, h_B is the coastal defence berm height evaluated at the toe of the dune or of the local defence, $h_1 = h + R_{up,2\%}$ is the total overtopping level ($R_{up,2\%}$ being the 2% exceedance level run-up) and $h_2 = h + \langle h_w \rangle$ is the total overflow level ($\langle h_w \rangle$ being the hourly average of set-up, run-up, and run-down contributions).
 160



3.2 Numerical weather and marine modelling system

The ensemble modelling system employed in this study to re-forecast the Vaia and Detlef storms and their effects on the Jesolo coast consists of a modelling chain that integrates the atmospheric WRF model, the hydrodynamic (ocean) SHYFEM model, the spectral wave model WAVEWATCH III (WW3), and the hydro-morphodynamic model XBeach. The sea levels at the coasts required to estimate *CFI* are directly computed by XBeach, which uses, as inputs, the nearshore sea levels and waves from SHYFEM and WW3. The latter are forced by the mean sea level pressure and surface wind speed from WRF-ARW, which downscales the IFS-ECWMF (i.e., the Integrated Forecasting System by the European Centre for Medium-range Weather Forecast) global medium-range ensemble weather forecast to a high-resolution, short-range, regional domain including the Adriatic Sea. The set-up of models is presented in the following.

3.2.1 Atmospheric model: WRF

Atmospheric downscaling of global weather forecasts is carried out using the Weather Research and Forecasting model (WRFV4.5.1). WRF is run on two two-way nested domains with horizontal resolutions respectively of 9 km, and 3 km (convection-permitting): the parent domain covering all Europe and the nested one centred over Italy (Figure 4). 65 vertical levels up to 50 hPa and a time step of 60 s are used. The parameterization used are (i) Multiscale Kain-Fritsch cumulus convection for the domain 1 only, (ii) Shallow cumulus GRIMS (Hong and Jang, 2018) for domain 1 only; (iii) Thompson for the microphysics for both domains; (iv) Mellor-Yamada-Janjic, TKE for the PBL; (v) Noah land – surface scheme; (vi) RRTMG for both short and long wave radiation; (vii) Eta similarity for the surface. The simulations are initialized using the 50 members of the Ensemble Prediction System (EPS) of the IFS-ECMWF plus the control member. For the Vaia event, the re-forecasts start at 00:00UTC on October 28, 2018 ending at 00:00UTC on Oct. 30. The re-forecasts for the Detlef event start at 12:00UTC on November 11, 2019 and they last for 48 hours ending on Nov. 13 at 12:00UTC.

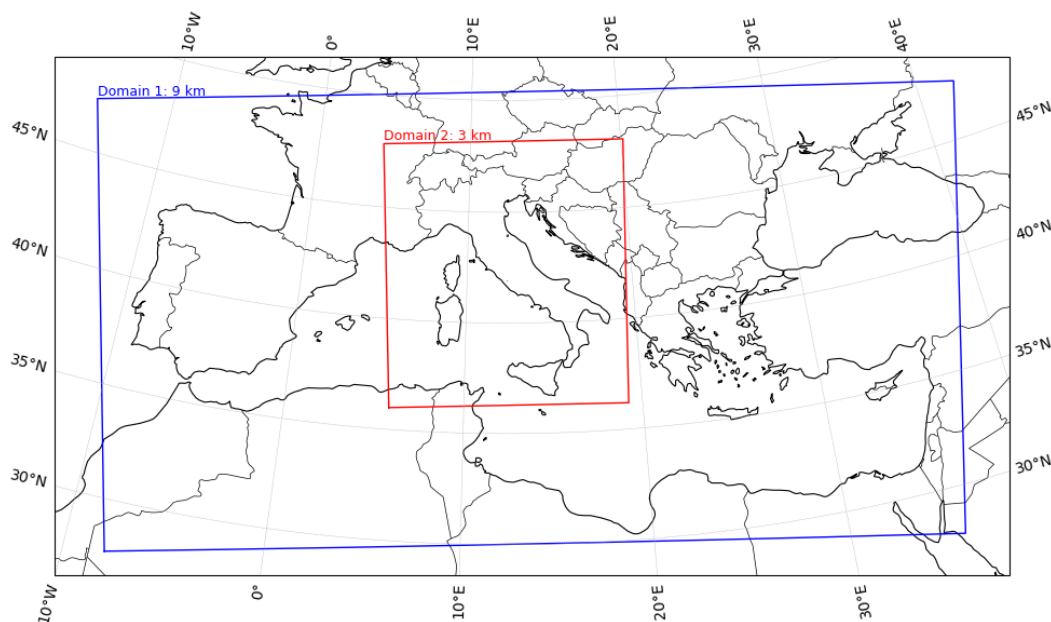


Figure 4: Numerical model domains used for the atmospheric WRF-ARW simulations. Domain 1 with a grid of 9 km (blue frame), Domain 2 with a grid of 3 km (red frame).

185 3.2.2 Coupled Ocean Wave model: SHYFEM + WW3

Sea-level and wave dynamics during pilot case storms Vaia and Detlef are re-forecasted using the finite-element hydrodynamic model SHYFEM (Umgiesser et al., 2022) coupled with the spectral wave model WAVEWATCH III (WW3; Tolman, 1991). The coupling accounts for several wave–surge interaction processes: 1) the contribution of waves to total sea level through wave setup and set-down; 2) the modulation of wave propagation by tides and storm surge, influencing refraction, shoaling, and breaking; 3) the effects of sea-level changes and currents on the propagation, generation, and dissipation of wind waves. In WW3, wind input and dissipation are parameterised with ST4 (Ardhuin et al., 2010), while nearshore bottom friction and depth-induced breaking processes through BT1 (Hasselmann et al., 1973) and DB1 (Battjes and Janssen, 1978).

Both the hydrodynamic and wave models operate on the same unstructured computational grid (Figure 5), which spans the entire Mediterranean Sea and consists of roughly 163,000 triangular elements. The unstructured mesh has a spatial resolution ranging from about 12 km in the open ocean to approximately 500 m along the coastline. Ocean-wave simulations are forced with 10-m wind fields (WW3 and SHYFEM) and mean sea-level pressure (SHYFEM) produced by the WRF atmospheric modelling system described above.

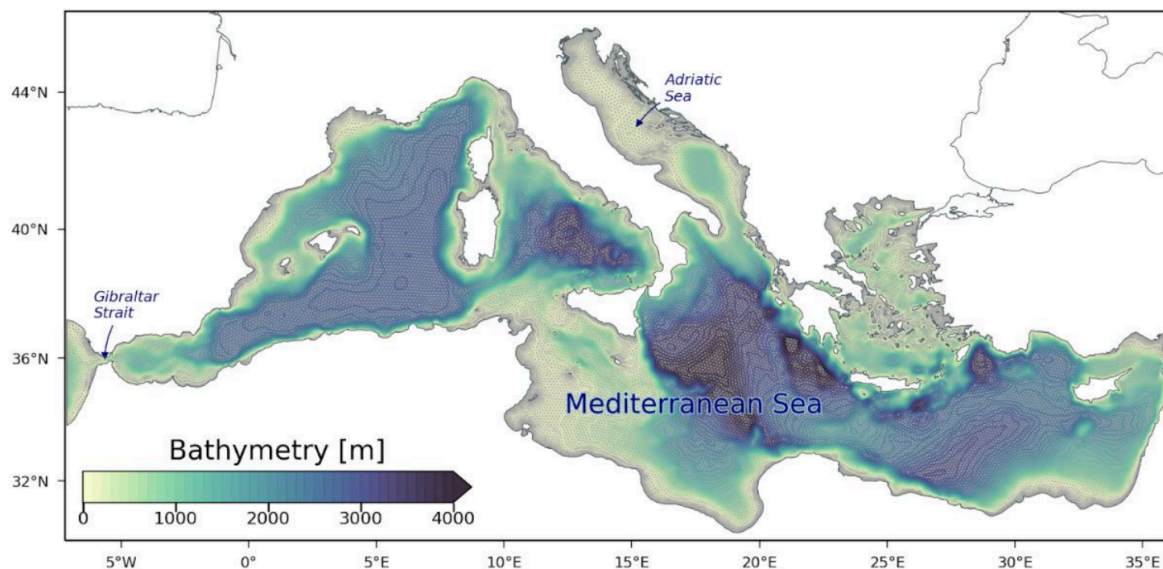


Figure 5: SHYFEM-WW3 unstructured computational grid.

200 3.2.3 Nearshore hydrodynamic model: XBeach

The wave set-up and run-up/run-down processes require modelling the nearshore area, either through analytical formulations (e.g., Stockdon et al., 2006) or by means of numerical models capable of reproducing nearshore dynamics. In the present study, we employ the XBeach model. XBeach is a two-dimensional depth-averaged (2DH) model that solves the coupled cross-shore and alongshore equations for wave propagation, flow, sediment transport, and bed level changes (Roelvink et al., 2009). For this study, XBeach is applied in a horizontally one-dimensional (1D) configuration, i.e., along a representative cross-shore transect, under the assumption of alongshore uniformity. This assumption is justified for the Jesolo case study, as the coastline is rectilinear and characterized by bathymetric contours approximately parallel to the shore, ensuring minimal alongshore variability. The 1D approach offers several advantages, including shorter computational times and reduced requirements for detailed alongshore bathymetric data. The model grid resolution ranges from 0.5 m in the swash region to 10 m at the nearshore boundary (located at -10 m depth, approximately 1800 m from the shoreline, Figure 6). The model is run in surfbeat mode (unstationary), which resolves the short-wave group-scale variations (short-wave envelope) and the associated long-wave oscillations. Sediment transport and morphological changes are not included in the simulations. All XBeach parameters are set to their default values, except for the wave breaking parameter ($\gamma = 0.42$), the threshold water depth above which cells are considered wet ($\epsilon_{ps} = 0.01$), and the depth of the run-up gauge ($rugdepth = 0.05$). These values are selected following Stockdon et al. (2014).

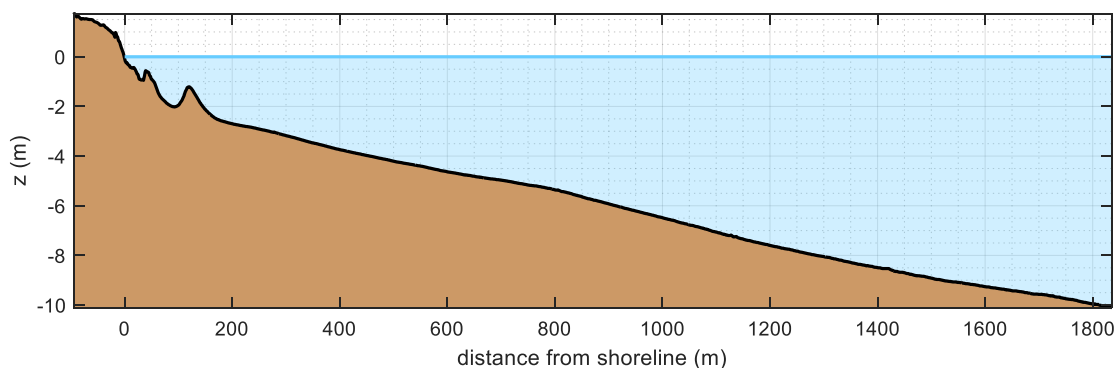


Figure 6: XBeach cross-shore profile.

3.3 Ensemble reduction

To achieve a relevant ensemble reduction, we draw here upon the methodology proposed by Molteni et al (2001), which were aimed at selecting only few Representative Ensemble Members (REMs) from a full ensemble to downscale global atmospheric forecasts to a regional domain, increasing the resolution thanks to the computational speed gain achieved after the ensemble reduction. Here we basically follow their two-step procedure that comprises (i) clustering of atmospheric variables on a space and time domain, and (ii) selection of the REMs. We hence refer the reader to Molteni et al (2001) for the details of these two steps. We focus here on the additions and modifications we have done to that methodology that proved to yield a better RENS relevance. In particular, we perform a dimensionality reduction of the input dataset for clustering, by feeding the clustering algorithm with the Principal Components of the dataset that explain the 80% of total variance (following, among others, Ferranti and Corti, 2011). This step is fundamental to support the clustering algorithm in properly clustering the samples (here, the 50 members) in presence of a much larger number of features (here, the number of grid points in space multiplied by the time steps considered). Indeed, we have found (not shown here) that RENS relevance increases with increasing explained variance until a certain level and then it quickly drops because the benefit of dimensionality reduction is lost.

The input for Principal Component Analysis (PCA) is a multivariate dataset composed of the IFS-ECMWF ensemble variables that are relevant for waves and sea level, namely: (i) 10-m wind speed components u and v , (ii) mean sea level pressure $mslp$, and (iii) squared wind speed U_{10}^2 as a proxy of the wind stress on the sea surface. These variables are selected on a restricted domain which entails the only Adriatic Sea, as the target area of this study is peripheral in the context of the Mediterranean Sea. Albeit the entire Mediterranean domain is needed to properly model the hydrodynamics in the target area (at least for the sea level, not necessary for waves), limiting the PCA and clustering to the semi-enclosed Adriatic Sea is necessary to properly represent the wind-driven processes that lead to storm surge along the northern littoral without taking into account what occurs in other, far and detached, Mediterranean basins. The full available time window (0 to 48-hour leadtime) is considered for PCA and clustering, sampling the fields with 6-hour intervals to represent the time trajectory of ensemble members while keeping the dataset within manageable size. The hierarchical agglomerative clustering is adopted



following Molteni et al (2001), but the Ward's minimum variance method (Wilks, 2011) has been preferred to the complete linkage because it yields to more relevant RENS (not shown here).

3.4 Ensemble statistics

245 In order to achieve a relevant ensemble reduction and provide a reliable flooding probability at the end of the modelling chain, we verify that RENS preserves the statistical characteristics of ENS. The statistics we consider here to that aim are the (i) ensemble mean, (ii) ensemble spread and (iii) the probability of flooding according to the *CFI* or other nearshore characteristics.

250 The mean is simply the average value over the ensemble members, while the spread is the standard deviation over the members. The global (i.e., over the full forecast range) probability of flooding at a target station, i.e., of a given *CFI* level, is estimated as:

$$P_{CFI} \approx N_{CFI}/N \quad (4)$$

255 where N_{CFI} is the number of ensemble members leading to a *CFI* level and N the total number of ensemble members. In this context, P_2 is the probability that $CFI = 2$, hence that there is flooding by overtopping in any of the time step in the forecast range. This measure provides information about the probability of a flood occurring but does not indicate when the flood is likely to occur. To determine how likely a flood will occur at time t , the temporal probability can be estimated as:

$$P_{CFI,t} \approx N_{CFI,t}/N \quad (5)$$

260 where $N_{CFI,t}$ is the number of ensemble members with *CFI* level at time t . A similar estimate can be obtained for the flooding probability $P_{\beta,t}$. The global and temporal probability of flooding can also be derived from RENS, and written in two ways:

$$p_{CFI} \approx \frac{\sum_{i=1}^n w_i}{N} \quad (6a)$$

$$\hat{p}_{CFI} \approx \frac{n_{CFI}}{n} \quad (6b)$$

265 the first accounting for the size w of the cluster each REM represents (e.g., $w_1 = 3$ if cluster number 1 is composed of 3 ensemble members) still remaining in the context of a N -member ensemble, the second based solely on the n REMs, which are equally weighted no matter the cluster size. Similarly, temporal probabilities of *CFI* levels ($p_{CFI,t}$ and $\hat{p}_{CFI,t}$) and of flooding ($p_{\beta,t}$ and $\hat{p}_{\beta,t}$) can be defined.



It must be stressed however that the probabilities in eq. (6) are not only different because they are based on a different sample space (n versus N), but they are also conceptually different. While in p_{CFI} every REM is weighted proportionally to the cluster size such that it approximates the full ensemble probability of CFI levels, \hat{p}_{CFI} is unweighted and answers a different question: *how likely is that one of the reduced ensemble scenarios leads to a certain CFI level?* In the context of early warning for coastal flooding, where the primary objective is to identify and forecast a range of plausible and potentially hazardous scenarios rather than to reproduce the full ensemble probability distribution, this question has been preferred. For this reason, all the analyses presented in the Results section (including the computation of ensemble mean and spread) are based on the unweighted approach, while the weighted approach is left for intercomparison and discussion in the Discussion section.

4 Results

4.1 Ensemble reduction

For both the storms, after a sensitivity analysis not shown here, the number of clusters and thus of REMs for the ensemble reduction is fixed here to 15, a number that represents a trade-off between the desired reduction with respect to 50 and a proper representation of the ensemble variability that is the better, the larger is n . Indeed, a 15-member RENS requires 30% of the numerical simulations required with ENS (the number of simulations scales linearly with n , leading to a potentially considerable reduction of the total computational time). At the same time the probability distribution of ENS is approximated by the 15 REMs, each representing other members. The REMs and their cluster weight (i.e., the number of members each REM is representative of, divided by the full ensemble size N) for the two storms are shown in Table 1.

Storm	Number of REMs	REMs (cluster weight)
<i>Vaia</i>	15	20 (16%), 47 (12%), 34 (10%), 30 (10%), 36 (10%), 13 (8%), 19 (6%), 16 (6%), 23 (4%), 29 (4%), 11 (4%), 9 (4%), 46 (2%), 0 (2%), 44 (2%)
<i>Detlef</i>	15	27 (12%), 21 (10%), 42 (8%), 1 (8%), 16 (8%), 13 (8%), 29 (8%), 3 (6%), 25 (6%), 12 (6%), 46 (6%), 8 (4%), 5 (4%), 39 (4%), 37 (2%)

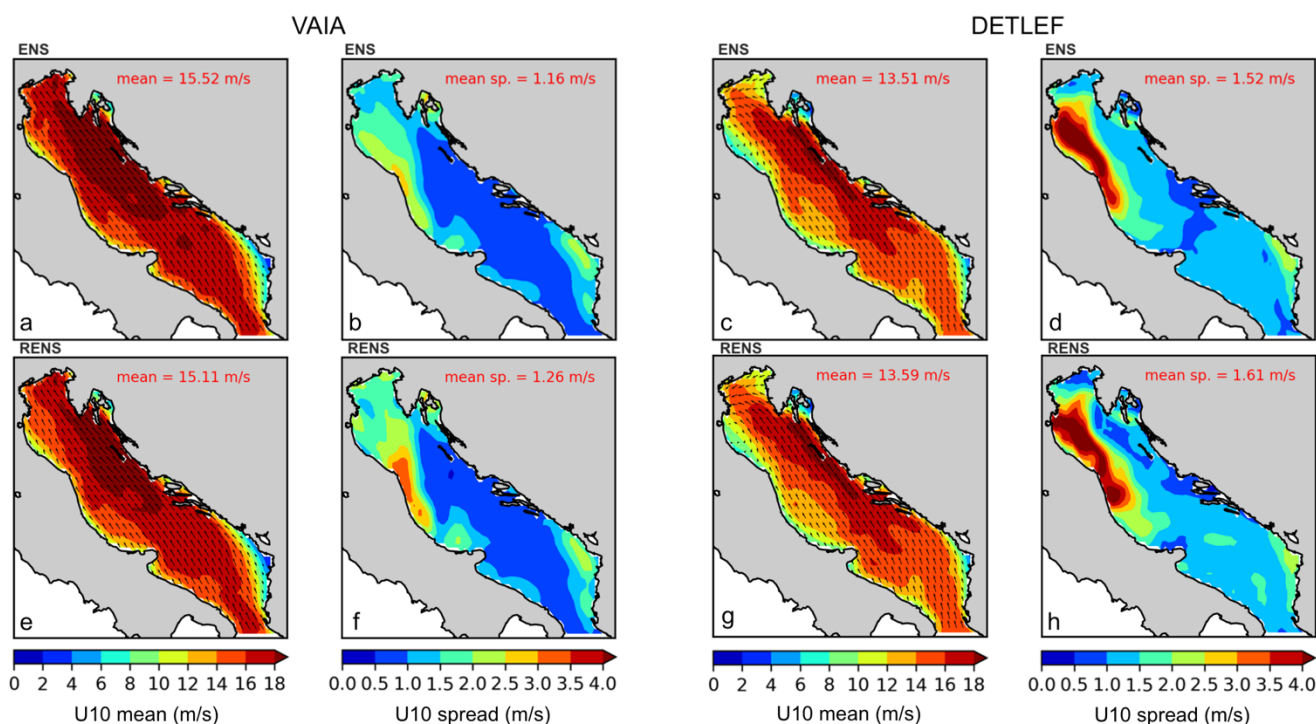
Table 1: Ensemble reductions for each of the two storm re-forecasts. Cluster weight is the number of members each REM is representative of, divided by the full ensemble size N (50).

The relevance of the reduction is assessed comparing the first two moments of ensemble statistics, i.e. mean and spread, from ENS and RENS. This is shown here for the wind speed (Figure 7), which is one of the clustering variables and one of the atmospheric forcings for the marine models SHYFEM and WW3, and for the sea level and significant wave height (Figure 8) at the nearshore location where the XBeach model takes its inputs.

In Figure 7, the magnitude and spatial variability of the ensemble mean wind field are well preserved by RENS for both the storms, with spatially-averaged mean U_{10} differing only marginally between ENS and RENS. The ensemble spread exhibits

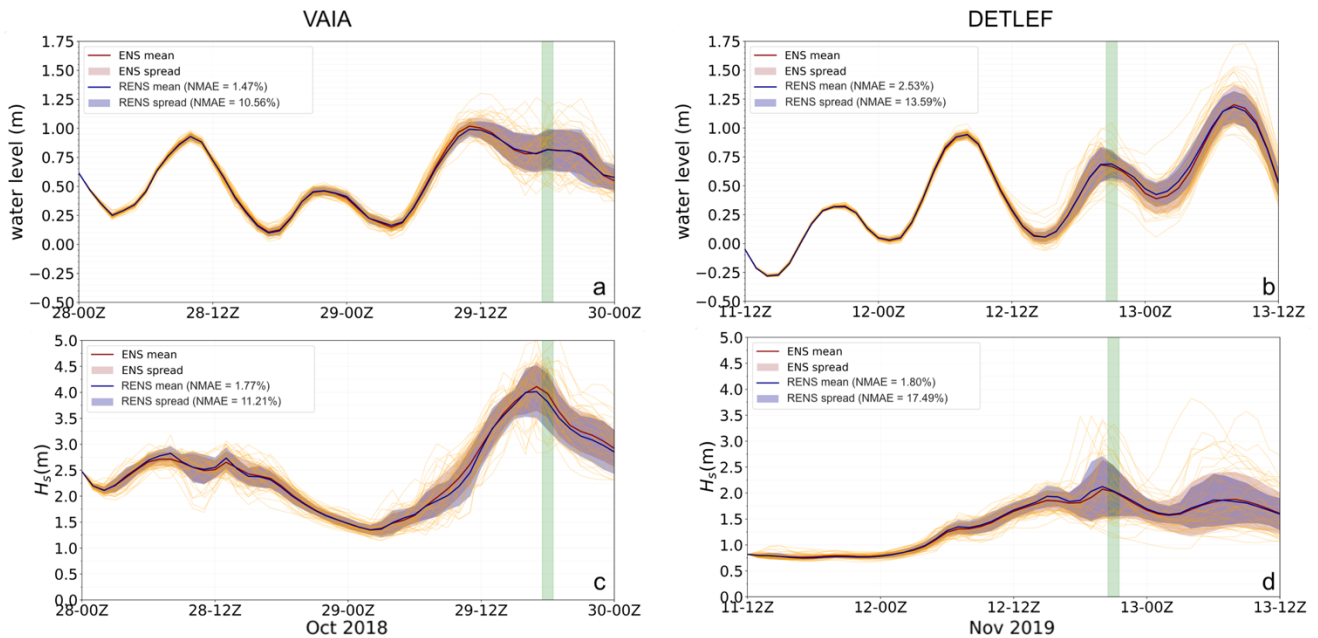


similar spatial patterns in both the storms, with maxima over the northern and central Adriatic Sea, associated with the strongest
 295 wind regimes. Small local differences in spread magnitude are visible, particularly during the Detlef storm when a small
 pressure minimum travelled northward increasing the forecast uncertainty, but the overall representation remains consistent
 between ENS and RENS (at the time step plotted in Figure 7: mean absolute relative difference for the ensemble mean 2.9%
 and 1.5%, for Vaia and Deflef, respectively; for the ensemble spread, 13.9% and 14.5%).



300 **Figure 7: Assessment of the ensemble reduction over the Adriatic Sea for Vaia (left, at 18UTC of 29/10/2018) and Detlef (right, at 18UTC of 12/11/2019) storms. Comparison of ensemble re-forecast from the complete ensemble (ENS, benchmark – top panels) and from the reduced ensemble (RENS – bottom panels): ensemble mean (panels a, e, c, g) and ensemble spread (panels b, d, f, h) of wind speed U_{10} .**

Figure 8 shows the comparison between ENS and RENS re-forecasts of water level (h) and significant wave height
 305 (H_s) at the nearshore site during the Vaia and Detlef storms. For both events, the temporal evolution of the ensemble mean and
 spread is closely reproduced by the reduced ensemble, with RENS capturing the timing and magnitude of the storm peaks.
 Minor differences between ENS and RENS are evident mainly around peak conditions, but they remain limited, as quantified
 by the low normalized mean absolute error (NMAE) values reported in the legends (smaller than 3% for the ensemble mean,
 smaller than 18% for the ensemble spread). The dispersion of individual ensemble members is also well represented, indicating
 310 that the ensemble reduction preserves the variability associated with forecast uncertainty. Overall, these results suggest that
 the reduced ensemble retains the essential information of the full ensemble for both water level and wave height during storm
 conditions.

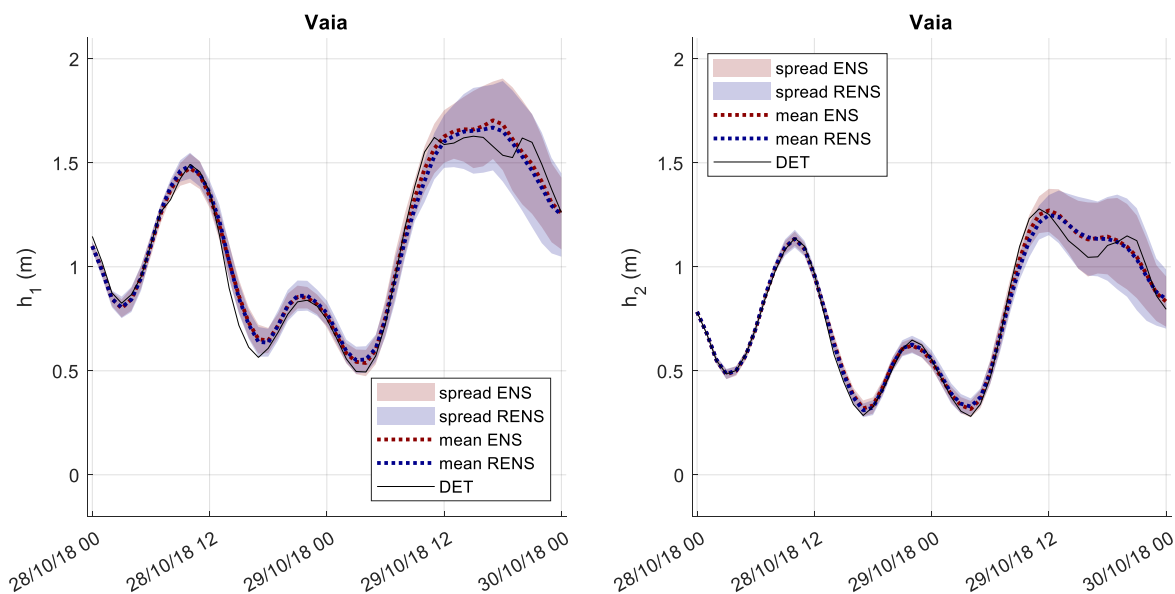


315 **Figure 8: Assessment of the ensemble reduction at the nearshore site, for Vaia (left panels) and Detlef (right panels) storms: water level h (panels a, b) and significant wave height H_s (panels c, d). Comparison of ensemble re-forecast (mean and spread) from the complete ensemble (ENS, benchmark - red color) and from the reduced ensemble (RENS - blue color, with Normalized Mean Absolute Error (NMAE) with respect to ENS within brackets in the legend): single ensemble members are drawn in orange color. The time of the event peak over the Venetian littoral is shaded in green colour. Spread area is considered as mean \pm 2spread.**

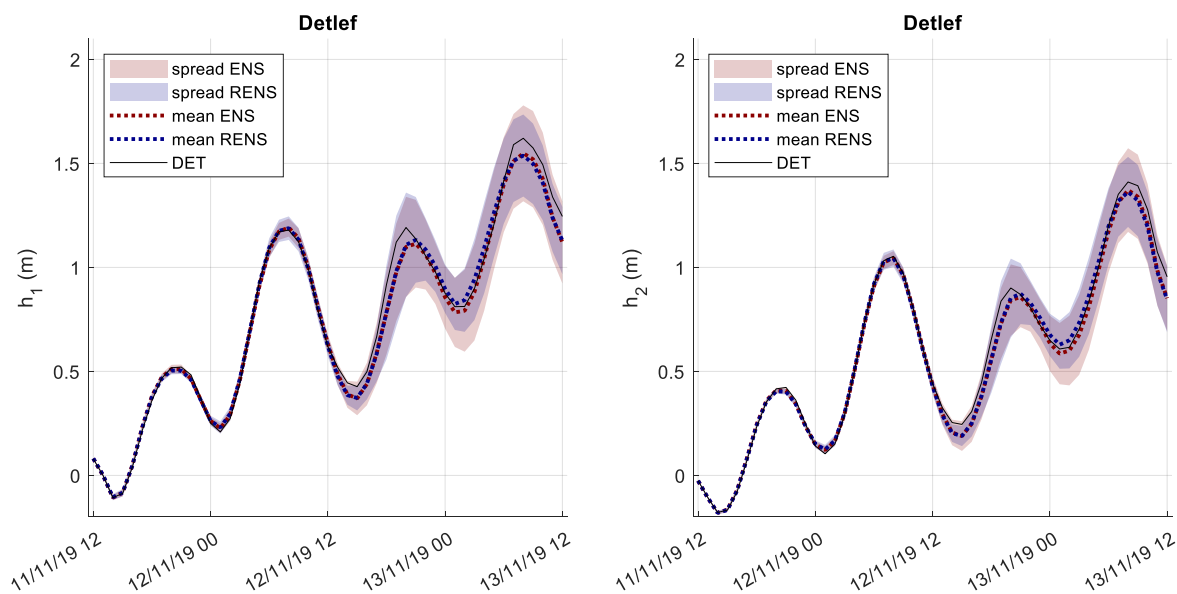
320 4.2 Coastal sea levels

The final stage of the ensemble modelling framework involves the application of the *CFI* to the pilot cases, with the aim of assessing its suitability as an early warning index and evaluating the performance of the ensemble reduction at this stage, with respect to the full ensemble on the one hand and with respect to the common deterministic forecast on the other. The assessment in the following is based on intercomparisons in terms of total sea levels, and duration and probability of coastal flooding.

325 Figure 9 and Figure 10 show the comparison between the ensemble (ENS, 50 members), the reduced ensemble (RENS, 15 members), and the deterministic (DET) re-forecasts of total sea levels at the beach during the Vaia and Detlef events, respectively, as computed with the XBeach model along a surveyed cross-shore profile of the Jesolo littoral. The shaded areas represent the forecast spread for ENS and RENS, while the dotted lines indicate their respective mean values. The deterministic re-forecast is shown as a dashed black line. Overall, the reduced ensemble closely reproduces both the mean behaviour and
330 the variability of the full ensemble. The deterministic re-forecast follows the general trend but does not account for the uncertainty represented by the ensemble approaches.



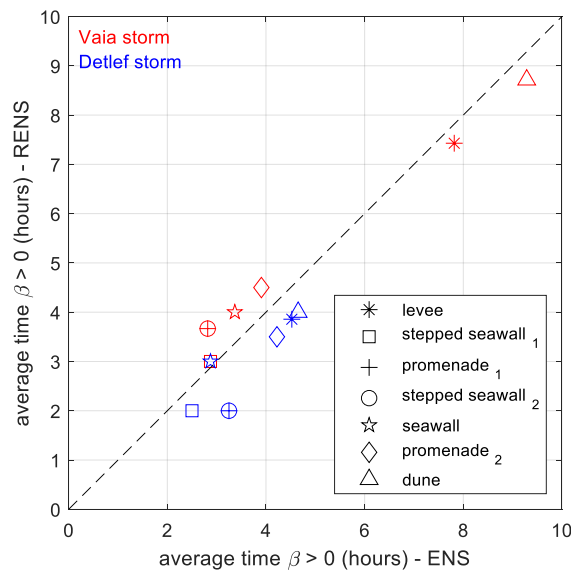
335 **Figure 9: Vaia storm - Comparison of ensemble re-forecasted total coastal sea levels (mean and spread) from the complete ensemble (ENS) and from the reduced ensemble (RENS): total sea level for overtopping h_1 (left) and total sea level for overflow h_2 (right). The black lines represent the deterministic control run. Spread area is considered as mean \pm 2spread.**





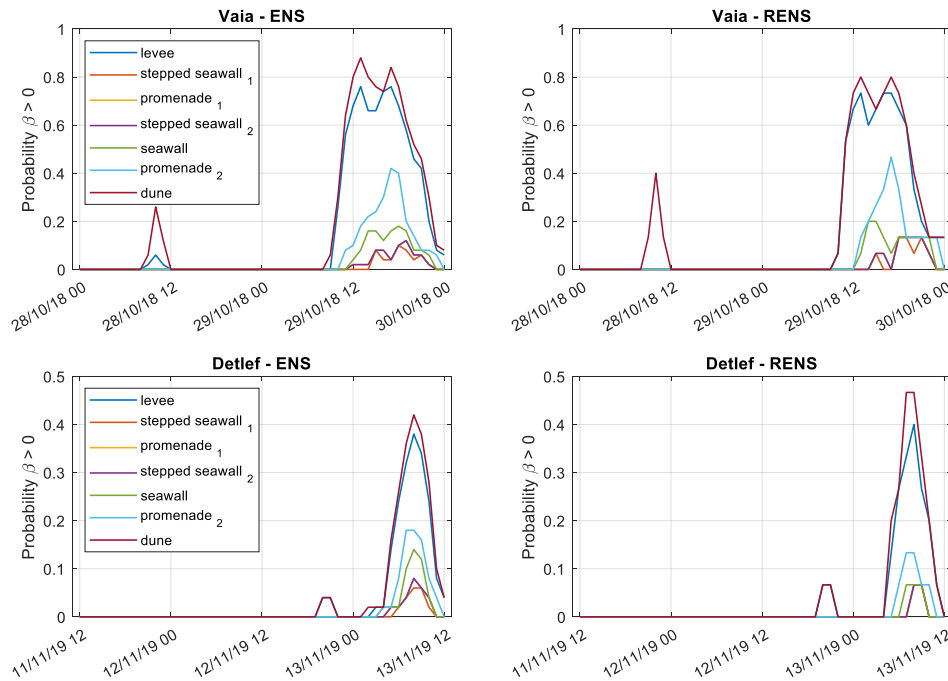
340 **Figure 10: Detlef storm - Comparison of ensemble re-forecasted total coastal sea levels (mean and spread) from the complete ensemble (ENS) and from the reduced ensemble (RENS): total sea level for overtopping h_1 (left) and total sea level for overflow h_2 (right). The black lines represent the deterministic control run. Spread area is considered as mean ± 2 spread.**

Figure 11 shows the comparison of the average duration of flooding above the emerged beach level (i.e. $\beta > 0$, corresponding to total sea level with swash exceeding the coastal defence berm height) obtained from ENS and RENS for the seven coastal defence structures along the Jesolo coastline (highlighted in Figure 1). Overall, a good agreement between ENS and RENS can be observed, with most of the structure markers close to the 1:1 line indicating perfect agreement. This indicates
 345 that the reduced ensemble is able to reproduce the temporal flooding characteristics with satisfactory accuracy. The deterministic re-forecast (DET) is not reported, as flooding ($\beta > 0$) occurs for only two structures and is limited to a duration of approximately one hour, thus preventing a meaningful comparison.



350 **Figure 11: Comparison of average flooding duration ($\beta > 0$), obtained using the complete ensemble (ENS, x-axis) and the reduced one (RENS, y-axis) for the seven coastal defence structures along the Jesolo coastline.**

Figure 12 shows the temporal probability of flooding (when $\beta > 0$) for the seven coastal defence structures along the Jesolo coastline, comparing RENS to ENS: RENS reproduces well the temporal flooding probability, including the timing of the onset, the peak, and the decay phase of the event. The behaviours among the different structures are generally consistent with those of ENS, although minor discrepancies can be observed, such as slight over- or underestimation of peak values and
 355 reduced variability for some structures.



360 **Figure 12: Temporal probability of flooding ($\beta > 0$) for the seven coastal defence structures along the Jesolo coastline, comparing the complete ensemble ($P_{\beta,t}$ – ENS, left panels) and the reduced ensemble ($\hat{p}_{\beta,t}$ – RENS, right panels) during the two storms. Note that some curves overlap: in the left panels, stepped seawall₂ overlaps promenade₁, while in the right panels it overlaps both promenade₁ and stepped seawall₁.**

4.3 Probabilities of coastal flooding

365 Figure 13 and Figure 14 show the flooding probabilities associated to the four *CFI* cases, for the seven coastal defence structures along the Jesolo coastline computed for the Vaia and Detlef events, respectively. For each structure, the stacked bars represent the relative probability of each *CFI* case, while the deterministic results are binary, indicating the occurrence of a single case only. Overall, the \hat{p}_{CFI} produced by RENS well represent the P_{CFI} obtained with ENS across all structures, preserving the relative importance of the different *CFI* cases. Minor differences can be observed for some structures, where RENS slightly under- or overestimates specific cases. For instance, for the Vaia storm, the ensemble approach consistently identifies the event as at least Case 2 across all structures (and in some instances as Case 3), thus correctly capturing the occurrence of relevant impact conditions. In contrast, the deterministic approach often results in lower-severity outcomes and would not have triggered an alert at 5 out of 7 structures, failing to capture the variability and uncertainty highlighted by the ensemble-based methods. These results emphasize the added value of ensemble forecasting in representing the range of possible coastal flooding cases, while confirming the capability of RENS to approximate the full ensemble behaviour with lower computational cost.

375

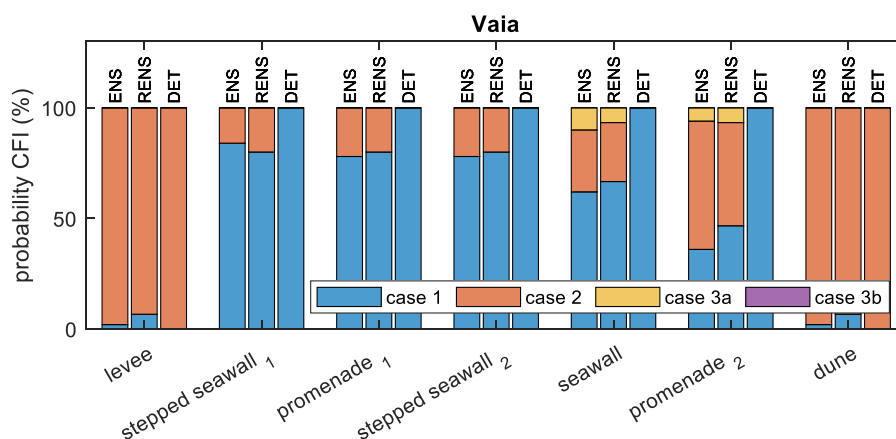


Figure 13: Vaia storm - Comparison of ensemble (ENS), reduced ensemble (RENS) and deterministic control run (DET) in terms of probabilities of the 4 CFI cases for the seven coastal defence structures along the Jesolo coastline. Probabilities are estimated according to eq. (4) for ENS and eq. (6a) for RENS.

380

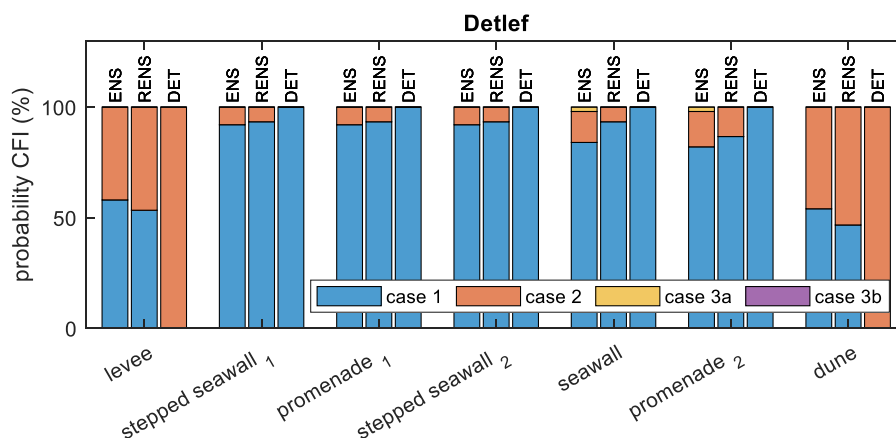


Figure 14: Detlef storm - Comparison of ensemble (ENS), reduced ensemble (RENS) and deterministic run (DET) in terms of probabilities of the 4 CFI cases for the seven coastal defence structures along the Jesolo coastline. Probabilities are estimated according to eq. (4) for ENS and eq. (6a) for RENS.

385 5 Discussion

The CFI and numerical modelling chain proposed in this study have been tested in a pilot case that consists of two storm events and a single site. Despite these events are well-studied as significant events that had recognized impacts on (and not only) the pilot site territory, of course our results and conclusions remain in the context of this framework, without any claim of

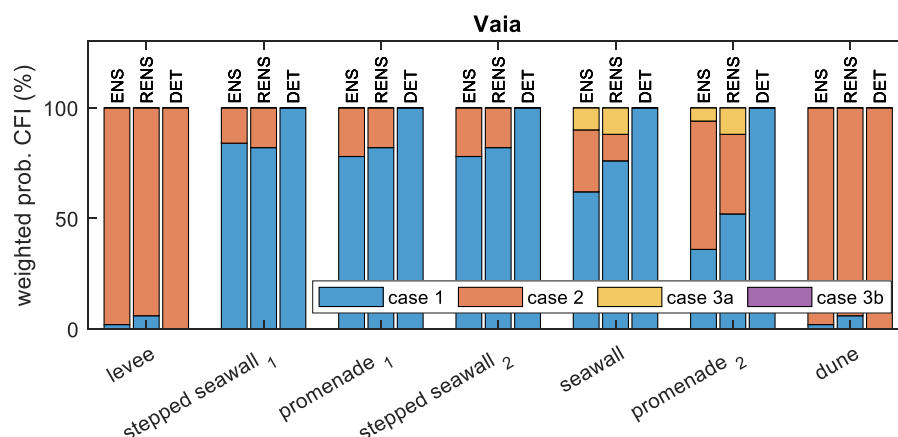


generality. This study is a proof-of-concept, demonstrating the potential of the tools employed in advancing the early-warning
390 of coastal flooding.

We have focused our attention on the relative performance of ENS versus RENS and both versus the deterministic
approach rather than on absolute forecast accuracy. Our modelling chain relies on state-of-the-art numerical models routinely
used in operational meteorological and marine forecasting. So, as a validation of the system is beyond our scope, we have
purposely not included any comparison of re-forecasts meteo-marine variables or coastal sea levels against observations. Doing
395 so, we are not required to discuss and manage the unavoidable forecast error in wind speed, mean sea level pressure, significant
wave height and sea level, which, however, is partially accounted for by the ensemble approach, at least for what concerns the
uncertainty due to initial conditions and nonlinear evolution represented by the ensemble spread. Most important, the validation
of ensemble-based forecasting systems is probability-based, thus requiring a much larger dataset than the one of our two pilot
case storms to be meaningful. Apart from this, it is not trivial to assess the *CFI* against observations because of, first of all, the
400 lack of flooding measurements and also the lack of knowledge of the effects of the uncertainty in the topography/bathymetry
and in coastal structure characteristics on the *CFI*. In general, the systematic measurement and the assessment of impacts is an
open topic and a gap to be filled in the development of impact-based forecasting systems and alerts.

Ensemble reduction was performed by clustering the ensemble members independently for each re-forecasted storm
and selecting one REM for each cluster. RENS was then defined as the set of REMs, and all ensemble statistics were computed
405 without weighting by cluster size (unweighted approach). This unweighted RENS should be interpreted as a scenario ensemble
rather than a probabilistic one, thought to sample the space of physically plausible and distinct forecasts, where each scenario
identified by the ensemble reduction contributes equally to the RENS statistics. Therefore, the comparison of P_{CFI} (ENS) and
 \hat{p}_{CFI} (RENS) presented in Figure 13 and Figure 14 is not intended as a validation of the unweighted probability, but as an
illustration of the differences between probabilistic (ENS) and scenario-based (RENS) interpretations of ensemble information.
410 The alternative approach consists in weighting each REM by the cluster size, thus approximating the probability density of the
full ensemble. While this weighted approach improves the reconstruction of probabilistic quantities, it partially reintroduces
information that is intentionally removed by the reduction procedure. As a consequence, weighted statistics tend to
underestimate the effective loss of ensemble spread associated with the dimensionality reduction, as less populated clusters,
often corresponding to low-probability but potentially high-impact scenarios, contribute marginally to the overall variability.

415 Figure 15 shows the weighted approach probabilities of the 4 CFI cases for the seven coastal defence structures during
the Vaia storm. The comparison between the unweighted (Figure 14) and weighted probabilities indicates that the differences
between the ENS and RENS configurations are generally slightly more pronounced in the weighted approach, reflecting its
sensitivity to cluster population and internal ensemble density. By contrast, the unweighted reduced ensemble yields more
consistent probability estimates, suggesting that the early-warning signal is primarily controlled by the presence of distinct
420 relevant scenarios rather than by their relative frequency within the full ensemble. However, Figure 15 also indicates that the
weighted approach might be adopted to deliver rather fair estimates of the probability of occurrence of coastal flooding.



425 **Figure 15: Weighted ensemble - Comparison of ensemble (ENS), reduced ensemble (RENS) and deterministic run (DET) in terms of probabilities of the 4 CFI cases for the seven coastal defence structures along the Jesolo coastline – Vaia storm. Probabilities are estimated according to eq. (4) for ENS and eq. (6b) for RENS.**

430 Finally, we have chosen to reduce the ensemble by means of a well-documented clustering technique rather than subsampling a number of members by simple random selection, which is another documented option (e.g., Serafin et al., 2019). However, we have preferred the clustering as it has been proved more effective than random selection in reproducing the statistical properties of the ensemble (Ferranti and Corti, 2011). In addition, it is computationally efficient and repeatable, it guarantees a better representation of the entire ensemble space including the less probable, but often most intense, scenarios and it can be as well set-up, as in our case, to deliver a reduced ensemble composed of real ensemble members rather than cluster centroids, keeping the physical consistence with the original dataset.

6 Final remarks

435 In this paper we have presented the proof-of-concept of an EW framework for coastal flooding forecast and alert, based on an ensemble modelling system integrating and coupling different components of the Earth System, from the atmosphere to the coast, and an EWI that we have called *Coastal Flooding Index (CFI)*. To reduce the computational burden of such a system, we have successfully explored and discussed the exploitation of an ensemble reduction based on clustering the ensemble members and using cluster representatives. Our aim was to demonstrate the feasibility of the approach and the potential for operational implementation of an ensemble-based EWS even by regional/local forecasting agencies also with limited computational resources, given the benefits of the ensemble reduction. We have tested the EW framework in a pilot case purposely chosen for the vulnerability of the low-lying sandy beach and close urbanised context and for the impact the Vaia and Detlef storms had on this territory. In doing so, we had no claim of generality, because we are well aware that a full operational validation of the system and of the *CFI* would require a systematic re-forecast covering a wide range of conditions and allowing a probabilistic-based assessment. It would also need, not secondary, coastal flooding measurements to build a

445



reference dataset. Such an experimental framework is not common, and it should be designed on purpose. We are aware of attempts of this in the same region, using numerical modelling of storm surge and waves together with coastal video monitoring. Including observations of the coastal flooding and of its impacts is certainly a potential follow-up of this study towards the full validation and an operational implementation.

450 In our pilot case, we have shown that reducing the ensemble from 50 to 15 members, thus considerably reducing the computational cost of forecasting (30% of numerical simulations required), does not significantly affect the probabilistic properties of the full ensemble when a guided clustering-based approach is adopted. The spatial patterns, time evolution, and magnitude of the ensemble mean and spread of wind speed, significant wave height, and nearshore sea level are consistently well represented by the reduced ensemble, with unavoidable local differences. This reflects in a comparably fair reduced
455 ensemble-based representation of the coastal flooding, including the coastal sea levels and their variability, and of its duration and probability. Considering the early-warning perspective, these flooding characteristics have been inter-compared among the deterministic-, reduced ensemble- and ensemble-based approaches, showing a fair agreement between the second and the third and pointing out the added values of them with respect to the first. Finally, the *CFI* level probability at the different coastal defense structures from the RENS and deterministic approaches have been benchmarked against the full ensemble
460 approach, showing that RENS can provide adequate and detailed coastal flooding alerts, improving the deterministic-based alerts solely limited to a binary outcome (flooding versus no flooding), but at the same time reducing the computational burden of a full ensemble system.

To summarize, this study has provided a proof-of-concept that probabilistic coastal flooding alerts based on complex numerical prediction systems, as the one here presented, can be compatible with the operational constraints of forecasting and
465 alert, when an impact-oriented index and ensemble reduction are combined. This framework is proposed as a good compromise between scientifically robustness and operational feasibility, building a solid base for future applications.

Code and data availability

Code and data used in this study are available upon request to the corresponding author.

Author contributions

470 CFa, and FB developed the methodology and analysed the study data. AR, MN and CFe performed the numerical simulations. FB, RF and CFa acquired and managed the resources and the funding that supported the study. CFa and FB prepared the manuscript. All co-authors contributed to the conceptualization of the study and to the editing of the manuscript.



Competing interests

The authors declare that they have no conflict of interest.

475 Disclaimer

Copernicus Publications remains neutral with regard to jurisdictional claims made in the text, published maps, institutional affiliations, or any other geographical representation in this paper. While Copernicus Publications makes every effort to include appropriate place names, the final responsibility lies with the authors. Views expressed in the text are those of the authors and do not necessarily reflect the views of the publisher.

480 Acknowledgements

The authors acknowledge the contribution by ECMWF through the 2025 Special Project “Exploiting Coupled, High-resolution modelling to simulate severe mediterranean cyclOgenesES (ECHOES)” that provided the computational resources for numerical simulations. AI tools were used to assist in the preparation of the abstract and to improve the fluency and clarity of selected sentences.

485 Financial support

This work was supported by the Italian Ministry of University and Research (MUR) under the PRIN-PNRR 2022 programme, funded by the European Union – NextGenerationEU, within the “PROtotype of Marine natural Hazard Early-warning sysTem based on Ensemble fOrecasting” (PROMETEO) project.

References

490

Ardhuin, F., Rogers, W. E., Babanin, A. V., Filipot, J., Magne, R., Roland, A., van der Westhuysen, A., Queffelec, P., Lefevre, J., Aouf, L., and Collard, F.: Semiempirical dissipation source functions for ocean waves. Part I: definition, calibration, and validation, *J. Phys. Oceanogr.*, 40, 1917–1941, 2010.

Battjes, J. A. and Janssen, J. P. F. M.: Energy loss and set-up due to breaking of random waves, in Proc. 16th Int. Conf. Coastal
495 Engineering, ASCE, 569–587, 1978.

Biolchi, L. G., Unguendoli, S., Bressan, L., Giambastiani, B. M. S., and Valentini, A.: Ensemble technique application to an XBeach-based coastal Early Warning System for the Northwest Adriatic Sea (Emilia-Romagna region, Italy), *Coast. Eng.*, 173, 1–19, <https://doi.org/10.1016/j.coastaleng.2022.104081>, 2022.



- 500 Cabrita, P., Montes, J., Duo, E., Brunetta, R., and Ciavola, P.: The role of different total water level definitions in coastal flood modelling on a low-elevation dune system, *J. Mar. Sci. Eng.*, 12, 1003, <https://doi.org/10.3390/jmse12061003>, 2024.
- Caruso, M. F. and Marani, M.: Extreme-coastal-water-level estimation and projection: a comparison of statistical methods, *Nat. Hazards Earth Syst. Sci.*, 22, 1109–1128, <https://doi.org/10.5194/nhess-22-1109-2022>, 2022.
- Cavaleri, L., Bajo, M., Barbariol, F., Bastianini, M., Benetazzo, A., Bertotti, L., and Umgiesser, G.: The October 29, 2018 storm in Northern Italy – an exceptional event and its modelling, *Prog. Oceanogr.*, 178, 102178, 2019.
- 505 Cavaleri, L., Bajo, M., Barbariol, F., Bastianini, M., Benetazzo, A., Bertotti, L., and Umgiesser, G.: The 2019 flooding of Venice and its implications for future predictions, *Oceanography*, 33, 42–49, 2020.
- Chatzistratis, D., Velegrakis, A. F., Chalazas, T., Alves, B., Schiavon, E., Monioudi, I., and Armaroli, C.: European Early Warning Systems for coastal floods: user needs, system availability and pertinent policy and legislation, *Int. J. Disaster Risk Reduct.*, 105, 105602, 2025.
- 510 Chondros, M., Metallinos, A., Papadimitriou, A., Memos, C., and Tsoukala, V.: A coastal flood early-warning system based on offshore sea-state forecasts and artificial neural networks, *J. Mar. Sci. Eng.*, 9, 1272, 2021.
- Favaretto, C., Ruol, P., and Martinelli, L.: Compartmentalization strategy for coastal flooding mitigation with application to a Northern Adriatic site, *Ocean Coast. Manag.*, 258, 107362, 2024.
- Ferranti, L. and Corti, S.: New clustering products, *ECMWF Newsletter*, 127, 6–11, 2011. Available at:
515 <https://www.ecmwf.int/en/elibrary/17442-new-clustering-products>
- Harley, M. D., Valentini, A., Armaroli, C., Perini, L., Calabrese, L., and Ciavola, P.: Can an early-warning system help minimize the impacts of coastal storms? A case study of the 2012 Halloween storm, northern Italy, *Nat. Hazards Earth Syst. Sci.*, 16, 209–222, 2016.
- Hasselmann, K., Barnett, T. P., Bouws, E., Carlson, H., Cartwright, D. E., Enke, K., Ewing, J. A., Gienapp, H., Hasselmann, D. E., Kruseman, P., Meerburg, A., Müller, P., Olbers, D. J., Richter, K., Sell, W., and Walden, H.: Measurements of wind-wave growth and swell decay during the Joint North Sea Wave Project (JONSWAP), *Ergänzungsheft zur Deutschen Hydrographischen Zeitschrift, Reihe A(8)*, 12, 95 pp., 1973.
- 520 IPCC: Climate Change 2023: Synthesis Report. Contribution of Working Groups I, II and III to the Sixth Assessment Report of the Intergovernmental Panel on Climate Change, Core Writing Team, H. Lee and J. Romero (eds.), IPCC, Geneva, Switzerland, 184 pp., <https://doi.org/10.59327/IPCC/AR6-9789291691647>, 2023.
- 525 Leijala, U., Björkqvist, J. V., Johansson, M. M., Pellikka, H., Laakso, L., and Kahma, K. K.: Combining probability distributions of sea level variations and wave run-up to evaluate coastal flooding risks, *Nat. Hazards Earth Syst. Sci.*, 18, 2785–2799, 2018.



- 530 Maragno, D., Pozzer, G., and Dall’Omo, C. F.: Supporting metropolitan Venice coastline climate adaptation: a multi-vulnerability and exposure assessment approach, *Environ. Impact Assess. Rev.*, 100, 107097, 2023.
- Molteni, F., Buizza, R., Marsigli, C., Montani, A., Nerozzi, F., and Paccagnella, T.: A strategy for high-resolution ensemble prediction. I: definition of representative members and global-model experiments, *Q. J. R. Meteorol. Soc.*, 127, 2069–2094, <https://doi.org/10.1002/qj.49712757612>, 2001.
- 535 Regione del Veneto: Aggiornamento dello studio: gestione integrata della zona costiera. Studio e monitoraggio per la definizione degli interventi di difesa dei litorali dall’erosione nella regione Veneto – Linee guida, Regione del Veneto, Venezia, Italy, 188 pp., 2023.
- Roelvink, D., Reniers, A., van Dongeren, A. P., de Vries, J. V. T., McCall, R., and Lescinski, J.: Modelling storm impacts on beaches, dunes and barrier islands, *Coast. Eng.*, 56, 1133–1152, 2009.
- Serafin, S., Strauss, L., and Dorninger, M.: Ensemble reduction using cluster analysis, *Q. J. R. Meteorol. Soc.*, 145, 659–674, 540 <https://doi.org/10.1002/qj.3458>, 2019.
- Stockdon, H. F., Holman, R. A., Howd, P. A., and Sallenger, A. H. Jr.: Empirical parameterization of setup, swash, and runup, *Coast. Eng.*, 53, 573–588, 2006.
- Stockdon, H. F., Thompson, D. M., Plant, N. G., and Long, J. W.: Evaluation of wave runup predictions from numerical and parametric models, *Coast. Eng.*, 92, 1–11, 2014.
- 545 Tolman, H. L.: A third-generation model for wind waves on slowly varying, unsteady, and inhomogeneous depths and currents, *J. Phys. Oceanogr.*, 21, 782–797, 1991.
- Turner, I. L., Leaman, C. K., Harley, M. D., Thran, M. C., David, D. R., Splinter, K. D., and Lowe, R. J.: A framework for national-scale coastal storm hazards early warning, *Coast. Eng.*, 192, 104571, 2024.
- Umgiesser, G., Ferrarin, C., Bajo, M., Bellafiore, D., Cucco, A., de Pascalis, F., and Arpaia, L.: Hydrodynamic modelling in 550 marginal and coastal seas – the case of the Adriatic Sea as a permanent laboratory for numerical approach, *Ocean Model.*, 179, 102123, 2022.
- United Nations (UN): Early Warning for All: the executive action plan, United Nations, available at: <https://www.un.org/en/climatechange/early-warning-for-all>, 2022.
- Wilks, D. S.: *Statistical Methods in the Atmospheric Sciences*, 3rd edn., Academic Press, Elsevier, Oxford, UK, 704 pp., 2011.
- 555 World Meteorological Organization (WMO): *WMO Guidelines on Multi-hazard Impact-based Forecast and Warning Services (WMO-No. 1150)*, World Meteorological Organization, Geneva, Switzerland, 2015.